Environmental Health Perspectives
Vol. 35, pp. 3-12, 1980

Chemical Modulation of Airway Epithelial Permeability

By R. C. Boucher*

The mucosal surface of the conducting airways has specialized structures for respiratory defense. Glands secrete mucus that may act as a barrier to particle penetration and participate in particle clearance. Intraepithelial irritant receptors aid in particle clearance through airway constriction and cough. The epithelium acts as a barrier to the penetration of inhaled material into the airway wall. Morphologic studies have identified the tight junctions adjoining respiratory epithelial cells as the principal barrier to passive solute translocation across the airway.

New approaches have been used to study airway epithelial function. Use of excised canine trachea mounted in Ussing chambers has permitted quantitative estimates of probe molecule permeation, the correlation of permeability with bioelectric properties, and estimation of equivalent pore radii. Probe molecule diffusion across canine trachea [mean transmucosal electric potential difference (PD) = 33 mV, lumen negative] is directly related to conductance (2.9 mS/cm^2) and is compatible with an equivalent pore radius of 7.5 nm. Direct measurement of tracheal PD in vivo (−29 mV) facilitates study of the genesis of the biopotential in intact animals. Measurement of the movement of HRP by radioimmunoassay has allowed correlation of the rate of probe flow across airway walls in vivo with ultrastructure. These approaches lend themselves to the study of pharmacologic and toxicologic effects on epithelial function. Antigen challenge, diethyl ether, and unfractionated cigarette smoke have been shown to increase epithelial permeability to HRP accompanied by ultrastructural evidence of tight junctional damage. Application of pharmacologic agents, e.g. amphotericin, ouabain, onto the respiratory epithelium induces similar changes in *in vitro* and *in vivo* PD. We conclude that techniques that have been used to measure permeability and transport in other epithelia may help elucidate modes of action of environmental agents on airways.

Epithelia generally exhibit two functions in organ homeostasis: they serve as a protective barrier, and they often possess specialized mechanisms of transport. As the control of ion and mucus secretion by the airway mucosa will be discussed later in this symposium, this presentation will focus on the role of airway epithelium as a barrier to passive translocation of large polar solutes — both as inhaled materials and resident macromolecules, across the airway. Previous work on the "barrier function" of the airway mucosa, predominantly morphologic, will be reviewed, and more recent approaches to the study of airway epithelial function that combine physiologic measures of airway permeability and morphology will be presented.

Until the late 1960s, it had been held that the respiratory epithelium was impermeant to protein macromolecules. Morphologic studies reported by Schneeberger and Karnovsky, employing horseradish peroxidase, a glycoprotein of ~40,000 daltons as an electron microscopic tracer, suggested that in the mammalian alveolus macromolecular flow across the epithelium was completely restricted at the level of the tight junctions adjoining alveolar pneumocytes (*1*). However, physiologic studies initially reported by Liebow et al. suggested radiolabeled albumin crossed the alveolar epithelium at sites that were not defined (*2*). These findings were confirmed by others (*3*). Little information on the movement of macromolecules across airway mucosa was available until 1973, when Richardson, et al. reported on attempts to localize within the airway wall inhaled protein antigens that elicited acute allergic bronchoconstriction in sensitized guinea pigs (*4*). These authors were unable to detect antigen, in this case HRP, below the epithelial tight junctions at times coincident with physiologic airway constriction. An hypothesis advanced for these results suggested that the rapid onset of bronchoconstric-

*Department of Medicine, School of Medicine, University of North Carolina, Chapel Hill, North Carolina 27514.

tion (~30 sec after initiation of challenge) involved antigen contact with mast cells residing in the airway lumen. Subsequent transmission electron microscopic (TEM) studies by Richardson et al. suggested that enzymatically intact HRP and ferritin do cross the guinea pig tracheal epithelium from airway lumen to interstitium (5). They concluded that this movement occurs via pinocytotic rather than paracellular routes and required at least 30-60 min for transfer; no preferential rates of movement of HRP (40,000 d) over ferritin (450,000 d) could be shown. Inoue and Hogg in subsequent studies concentrated on defining the ultrastructure of the epithelial tight junctions (6). Freeze fracture studies from guinea pig trachea revealed a junctional compartment that is relatively deep — ca. 0.5 mμ — and composed of an average of seven strands, interconnected to form compartments.

Studies of respiratory epithelial permeability to macromolecules have been hampered by several technical problems. Satisfactory probe macromolecules for use in estimating the permeability of relatively tight or impermeable epithelia have been lacking. Radioactive label from externally labeled probes often elutes or is cleaved from the parent compound. Because of the restrictive sieving characteristics of respiratory epithelia, flows of the lower molecular weight-free label or labeled fragments across the barrier will dominate and yield erroneously high permeability coefficients. In the worst cases, free label can bind to resident macromolecules, e.g., albumin, making evaluation of the nature of the permeant radioactivity by common techniques, e.g., TCA precipitation, impossible. Such considerations have similarly hindered combined morphologic-physiologic studies of macromolecular translocation in respiratory epithelia. Such techniques as radioautography have been relatively disappointing for these purposes, because there is little evidence that radioactivity faithfully reflects location of probe molecules.

These considerations led to the development of sensitive techniques to monitor the movement of the EM tracer horseradish peroxidase (HRP) across relatively impermeable barriers. Because of the need to use small amounts and low concentrations of this material on mucosal surfaces, an assay sensitive to nanogram/ml quantities of HRP in plasma was required. As the presence of circulating endogenous peroxidases rendered the enzymatic determination of HRP in plasma at low concentrations unreliable, a solid-phase radioimmunoassay (RIA) that detects HRP in plasma to concentrations of 10 ng/ml was developed. After application of small volumes of HRP onto the airway mucosal surfaces, rate constants of HRP transfer into blood can be estimated and routes of HRP movement across the epithelium examined morphologically with the transmission electron microscope.

Early studies showed that after instillation of 1 mg of purified HRP into guinea pig trachea, a small fraction of the instilled HRP was measurable in plasma 10 min later (0.08% instilled dose) and that the rate of HRP accumulation in plasma was relatively constant from 10 to 40 min (Fig. 1). To assess effects of an inspired agent on tracheal permeability, the following protocol was utilized: after control blood samples were obtained, 1 mg of purified HRP in 0.2 ml PBS was instilled onto the tracheal surface through a tracheostomy tube. Blood was sampled for HRP by RIA at 10, 15, and 20 min, with the rate of accumulation in plasma over this interval calculated by the least-squares method. After the 20 min measurement, an inhalation exposure to a test agent was administered and post-challenge rates of HRP accumulation in plasma determined from 20-40 min measures of plasma HRP. The significance of aerosol-induced rate changes was estimated by comparing these rates for individual animals within each group with paired *t*-tests. At various points within this time frame, animals were sacrificed and HRP localized in mucosal tissue on transmission electron micrographs. In addition, respiratory parameters, tidal volume, dynamic compliance, and pulmonary resistance, as well as arterial blood gases and blood pressure, were measured with the animal in a pressure sensitive plethysmograph to provide an index of more traditional physiologic effects of the inspired agent.

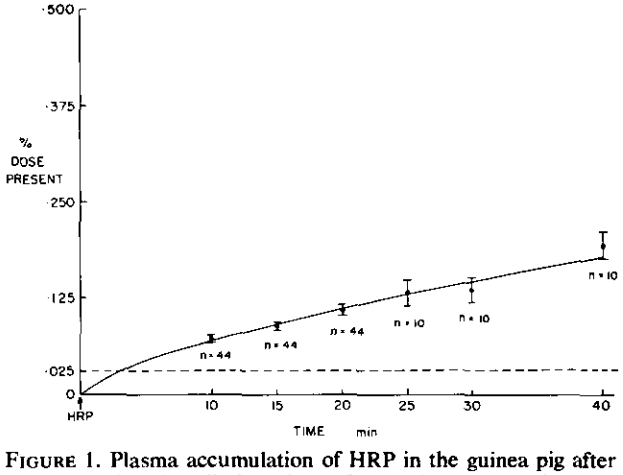

FIGURE 1. Plasma accumulation of HRP in the guinea pig after intratracheal installation of 1 mg HRP. The ordinate gives the fractional plasma absorption of instilled HRP.

We have recently reported data assessing the sensitivity and validity of this methodology for measuring changes in protein transport in the tracheobron-

chial mucosa (7). In control studies, it was found that sham challenge with air did not change HRP plasma accumulation rates, and electron micrographs at 23 and 40 min after HRP instillation showed HRP to be localized primarily atop the mucous barrier, suggesting that the instillation technique did not induce mucosal trauma or direct toxic effects. In contrast, diethyl ether exposure, which Richardson et al. had shown morphologically to induce HRP penetration into guinea pig tracheal epithelium, led to a threefold increase in rate of plasma HRP accumulation. Electron micrographs confirmed Richardson's observations that HRP was present in the proximal intercellular spaces, a finding that could result from a loss of the barrier function of the tight junctions. A similar association between increased flow of HRP from lumen to blood *in vivo* and loss of the barrier function of the tight junction has been reported in the gut (*8*). Gel filtration of plasma from control and exposure animals showed the HRP measured in plasma by RIA to be intact 40,000 d protein with no smaller molecular weight fragments measurable.

More recently, in collaboration with Ms. Joy Johnson in Montreal and Dr. Hogg, these techniques have been used to pursue earlier morphologic observations of Simani et al. that inhalation of cigarette smoke increases HRP penetrance into guinea pig epithelium (*9, 10*). In these studies, guinea pigs, 20 min after intratracheal instillation of HRP were assigned to one of five exposure groups: (1) a control group exposed to 20 puffs of air; (2) a group exposed to 5 puffs of whole cigarette smoke; (3) a group exposed to 20 puffs of whole smoke; (4) a group exposed to 100 puffs of whole smoke; and (5) a group exposed to 100 puffs of smoke that had been passed through a standard Cambridge filter pad, effectively removing the particulate phase of smoke, thus exposing the animal to the "vapor" phase of smoke. Smoke or air was delivered to the animals by a specially designed smoking machine that, from standard flue cure cigarettes, delivered 20 ml puffs of smoke into a length of tubing that was attached to the inspiratory port of the tracheostomy tube. The results for control, post exposure rates, and p values for these groups are shown in Table 1. For the control group the mean rate of HRP accumulation after air exposure, while moderately lower, did not differ statistically from the control (10-20) period. Five puffs of whole smoke has relatively little effect on rates of HRP accumulation while the mean rate of plasma HRP accumulation after 20 puffs of smoke was moderately increased, principally due to a variable effect at 40 min. It can be seen that 100 puffs of whole cigarette smoke resulted in about a threefold rise in the rate of plasma HRP accumulation over control, an increase significant at the $p < 0.01$ level.

Table 1. Rates of plasma HRP accumulation for control periods and after exposure to graded doses of cigarette smoke.

	Rates of HRP accumulation, % delivered dose/min			Ratio
	10-20 min	20-40 min	P	20-40 / 10-20
Control (N=14)	0.0053	0.0038	NS	0.7
5 puffs (N=12)	0.0055	0.0053	NS	1.0
20 puffs (N=11)	0.0055	0.0099	0.09	1.8
100 puffs (N=15)	0.0048	0.0122	<0.01	2.5

In addition to standard transmission electron microscopic studies, freeze fracture studies were performed by Sada Inoue on tracheal epithelium from guinea pigs that inhaled equivalent amounts of smoke. In contrast to the normal morphology as revealed by this technique, beading and disruptions of the fibrils, loss of discrete compartments and free fibrillar endings were noted after smoke inhalation. While the precise relationship between the morphology of the junction as revealed by freeze fracture techniques and probe permeation is controversial, the changes are consistent with the TEM evidence of damaged tight junctions and the increases in probe (HRP) flow.

Figure 2 shows the application of these techniques to identify the noxious components of cigarette smoke. This figure shows that exposure to 100 puffs of the vapor phase of cigarette smoke — that is, whole smoke passed through a Cambridge filter — is not associated with increased rates of plasma accumulation of HRP over control. These data suggest that the tars and nicotine in the particulate phase, rather than the acroleines, CN^- and NO_X in these vapor-phase exposures, are likely to be the active agents. Data consistent with these observations have

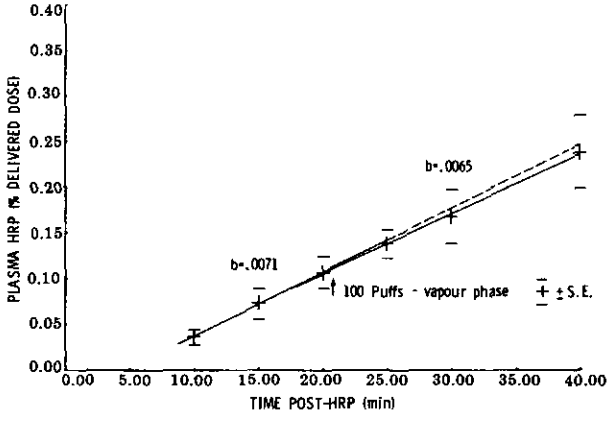

FIGURE 2. Rate of plasma HRP accumulation before (b=0.0071% delivered dose/min) and after (b=0.0065%/min) exposure to vapor phase of cigarette smoke.

recently been obtained showing that high tar, high nicotine cigarettes produce significantly greater increases in tracheal permeability to HRP than low tar, low nicotine cigarettes.

In summary, this technique has been useful in measuring the changes induced by inhaled agents in tracheal mucosal permeability to an intact macromolecule, HRP, and in identifying morphologic sites of mucosal damage.

However, the protocol has raised questions about the normal routes of HRP movement across the airway mucosa. As noted earlier, Richardson et al. suggested HRP moves across guinea pig tracheal mucosa via pinocytosis relatively slowly, i.e., requiring 30-60 min. However, in our experiments HRP was easily measurable in plasma 10 min after instillation. Electron micrographs taken at these early intervals, like those of Richardson et al., failed to show HRP penetration into the lateral intercellular spaces or basal areas. A similar discrepancy between the rate of HRP movement across the pulmonary capillary to lymph duct, and electron microscopic evidence of tracer egress from capillary lumen, has recently been reported (*11*). These observations imply that standard EM techniques may not be sufficiently sensitive to detect a small number of HRP molecules traversing the tight junction or are unable to detect transport via a small number of vesicles emptying into the lateral or basal areas of the epithelium. Alternatively, localized areas of transport such as the bronchus-associated lymphoid tissue (BALT) (*12*) areas or increased cell turnover may be missed by the sampling procedure.

In order to better describe the movement of macromolecules across airway epithelium, precise measurement of translocated probes and the surface area available for permeation are necessary. *In vitro* studies with excised trachea mounted in Ussing chambers, as first reported by Olver et al., have proved useful for such studies (*13*). In these experiments, epithelium from the posterior membrane of canine trachea is mounted as a flat sheet between two Lucite half chambers. The bathing solutions, generally Ringer's or Krebs-Henseleit, are gassed, circulated, and warmed. In most situations, these solutions are identical on both sides of the membrane, eliminating chemical and hydrostatic pressure gradients. Via sensing bridges closely apposed to each surface of the membrane, transmural PD is recorded with a voltmeter. The membrane can be shortcircuited, that is, the transepithelial PD reduced to zero, by imposing the EMF of an external battery across the membrane via a second pair of bridges. The current through the external circuit short circuit current (I_{SC}) is recorded on an ammeter. Because this tissue behaves like an ohmic resistor, resistance R and its reciprocal, conductance G, can be calculated from the I_{SC} and open circuit potential difference (PD). For our studies, probe molecules, which differed in size, but too large to enter the intracellular space, were added to the mucosal bathing solution and the rate of probe appearance in the serosal solution was monitored by tracer counting (^{14}C-mannitol, ^{3}H-inulin) or RIA (HRP) (*14*). Permeability coefficients for these probes were calculated.

The bioelectric properties of canine trachea measured in these studies were similar to those reported by Olver et al. (Table 2). Probe molecule addition, particularly HRP, at a dose of 7.5 mg/ml, did not change bioelectric properties. Rates of entry into the sink were linear 30 min after the molecules were added to the source.

Table 2. *In vitro* bioelectric properties of excised canine trachea in Ussing chambers.

	Bioelectric properties[a]	
	Present study	Olver et al. (*13*)
PD, mV	33.5 ± 2.9	30.7 ± 2.7
I_{SC}, μA/cm^2	97.6 ± 11.0	108.0 ± 8.0
G, (mS/cm^2)	2.91 ± 0.18	3.51

[a]Mean ± SE.

From the data of Marin et al. it can be calculated that the electrical G (3.3 mS/cm^2) approximates the sum of $J_{Cl^-}^{M\to S}$ (2.4 mS/cm^2) and $J_{Na^+}^{S\to M}$ (1.4 mS/cm^2), i.e., $\Sigma J_{Na,Cl}^{passive} = 3.8$ mS/cm^2 (*15*). Further, permeability coefficients for Na^+ and Cl^- can be calculated from these fluxes. The ratios of P_{Cl^-} and P_{Na^+} to P_{man}, 3.2 and 1.6 respectively, approximate the aqueous free diffusion ratios: $D_{Cl^-}/D_{man} = 2.8$; $D_{Na^+}/D_{man} = 1.9$. Because mannitol is assumed to move through extracellular paths, the similarity in the permeability ratios and the ratio of the free diffusivities suggest passive Na and Cl movement is unrestricted and occurs largely via aqueous paracellular routes.

The permeability coefficients of the respiratory mucosa *in vitro* to probe solutes, the ratios of P_{probe} to P_{man}, and free diffusion ratios of D_{probe} to D_{man} are shown in Table 3. The comparison of permeability coefficients is one of the methods that has been used by Solomon and others to calculate equivalent pore radii (*16*). In this analysis, $P = F(a/r)D/\Delta X$, where

$$F(a/r) = (1 - a/r)^2 [1 - (2.1a/r) + (2.09a/r^3) - (0.95a/r^5)]$$

and a = probe molecule radius, r = pore radius, and ΔX = path length.

Comparison of the permeability coefficients for probe molecules to a common reference, i.e.,

$$\frac{P_X}{P_{ref}} = \frac{F(a_X/r)}{F(a_{ref}/r)} \frac{D_X}{D_{ref}}$$

eliminates the path length. The results of such an analysis are shown in Figure 3. As the molecular radius of the probe molecule increases, the permeability coefficient, relative to that of mannitol, decreases. The direction of this change is predicted for movement in free solution. However, the ratios for inulin and, particularly HRP are smaller than those predicted for free diffusion suggesting that the movement of these molecules is restricted and that the barrier behaves like a "sieve." A single equivalent pore of 75 Å appears to fit our data. Although this pore size may seem relatively large in the light of published comments on the relationship between PD, conductance, and the "tightness" of epithelia (*17*), the total pore area can be calculated to occupy 0.05% or less of total surface area. The presence of albumin, a macromolecule of similar size to HRP, in canine airway liquid (*18*) obtained *in vivo* from normal dogs suggests that these paths are present under physiologic conditions.

It should be noted that the electrical conductance G reflects current that is carried by small ions. The magnitude of the conductance may reflect the total area of the aqueous channels in the barrier but the magnitude of restricted diffusion or apparent pore dimensions cannot be predicted directly from G.

The existence of size-dependent restriction or "sieving" solutes across tracheal epithelium implies movement through paracellular pores rather than by pinocytosis. Other evidence supports this hypothesis. The rate of flow of probes was directly related to tissue conductance, indicating movement of these solutes by the same paracellular paths as ions. The unidirectional fluxes of the probes were symmetric, i.e., flow from S→M equalled flow from M→S, as would be anticipated for a diffusional process. Finally, in collaboration with Dr. N. S. Wang of McGill, samples of the tissues were examined ultrastructurally and vesicles were not detected.

Edge damage, i.e., chamber-induced membrane damage, is a concern in all experiments where tissue is clamped between two chambers. Although rigorous analyses of edge effects have not been reported in this tissue, varying edge to surface area ratios, varying edge compression, and comparison of bioelectric properties obtained with our apparatus to those in the literature, including "edge-free" systems, suggest no substantial edge artifacts in these experiments. As edge-induced increases in G might be expected to decrease PD measured *in vitro*, comparisons of *in vitro* PD to measurements of PD made directly *in vivo* in canine trachea, if similar, would

Table 3. Permeability of canine tracheal epithelium to solutes *in vitro*.

Probe solute	Canine trachea		Free diffusion
	$P \times 10^7$, cm/sec	P_{probe}/P_{man}[a]	D_{probe}/D_{man}
$^{36}Cl^-$	52[b]	3.2	2.8
$^{22}Na^+$	25[b]	1.6	1.9
^{14}C-Mannitol	16	1	1
^{3}H-Inulin	4.4	0.25	0.33
Horseradish peroxidase	0.1	0.006	0.076

[a]Calculated from the contemporaneous fluxes of mannitol and the probe across the same preparation (except for Na^+ and Cl^- permeation through dog trachea).

[b]Calculated from the lumen to serosa flux of Cl^- and the serosa to lumen flow of Na^+ reported by Marin et al. (*15*).

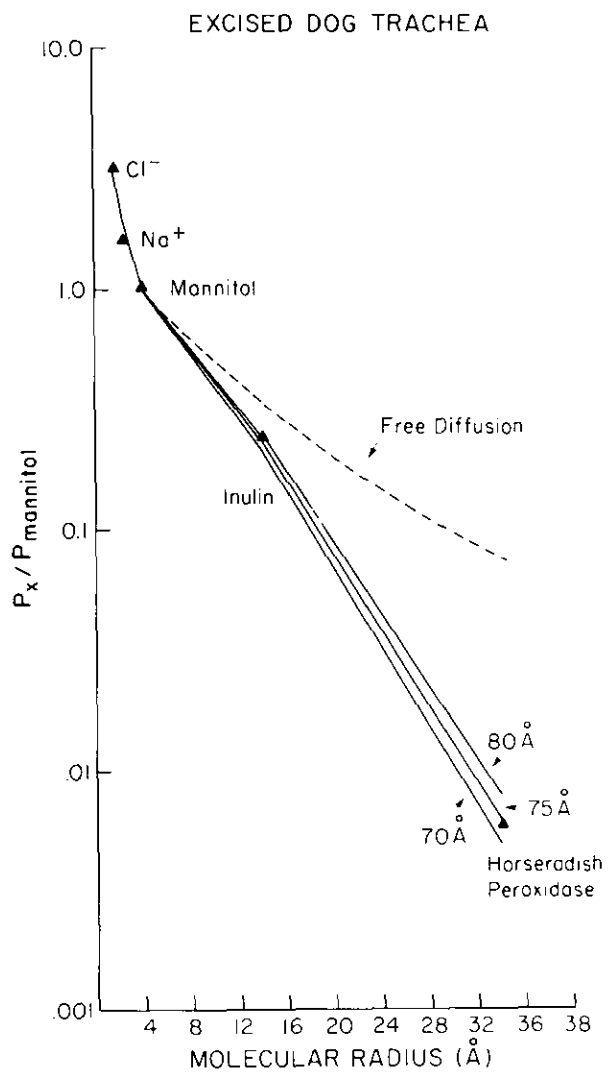

FIGURE 3. Semilogarithmic plot of ratio of P_{probe}/P_{man} versus molecular radius. Solid lines show predicted values for equivalent pore radii 70-80 Å.

also suggest no substantial edge artifacts.

As reviewed above, the bioelectric properties of excised canine trachea can be measured in Ussing-type chambers, which permits the study of the tissue under short circuit conditions, i.e., no electrochemical driving force for solute movement. Under these conditions and with no hydrostatic gradient, asymmetric unidirectional fluxes of a tracer species (i.e., net flow) is primary evidence for active transport. Olver and Marin have demonstrated Cl^- secretion and a smaller Na^+ absorption across the short-circuited canine trachea (*13*). As shown in Table 1, the canine trachea exhibits an average peak PD of ~30 mV—lumen negative—and an I_{SC} of 75-100 $\mu A/cm^2$. The radiotracer studies suggest that the open circuit PD is generated by active ion transport mechanisms that were identified under short circuit conditions. Several pharmacologic agents that were added to the solutions that bathed canine trachea *in vitro* have been shown to alter bioelectric properties and ion fluxes.

However, the relevance of the *in vitro* model to *in vivo* function, both for our studies and salt and water metabolism, hinges on the similarities in the basic properties of the two preparations. The selection of appropriate bioelectric properties for comparison is not obvious since the time course of PD *in vitro* is complex. After mounting, transepithelial PD transiently falls but subsequently gradually rises to reach a relatively stable plateau 1-2 hr after mounting. We and others have selected this plateau value as the value likely to represent the PD of the epithelium *in vivo*. To verify this supposition and because Hale et al. have reported an *in vivo* canine tracheal PD of only −5 mV, we have developed a technique to measure PD directly *in vivo* (*19, 20*).

The protocol is begun by balancing the reference electrode — a 19 gauge needle containing Ringer 4% agar — and the fluid-filled exploring bridge (PE-160 tubing) in a common reservoir of Ringer. The calomel electrodes connecting these bridges to the voltmeter were selected to have an offset potential of <1 mV for each study. Adult male mongrel dogs, mean weight 18 kg, were anesthetized with IV pentobarbital sodium or amylbarbital and intubated. The reference electrode was placed in a subcutaneous space, which had been shown in preliminary studies to be isoelectric with the serosal surface of the trachea. The exploring electrode was advanced through the endotracheal tube. Contact with the tracheal surface was insured by continuous perfusion through the bridge at 0.1 ml/min. with warmed, gassed Ringer solution. The potential sensed by this bridge was transmitted to the calomel half-cell via Ringer 4% agar bridge that connected the perfusion reservoir with the cell.

The calomel electrodes were connected to a high impedance volt-meter, filtered to remove 60 cycle interference, and values displayed digitally and recorded on a strip chart.

Figure 4 shows representative tracings obtained by use of the fluid filled bridge. It can be seen from the top tracing with relatively fast paper speed that the PD recorded from this dog is stable but shows oscillations which correspond to respiratory movements. The bottom tracing shows a 6-min interval indicating stability of tracing. Continuous tracings are stable, within 10%, over periods of at least 30 min.

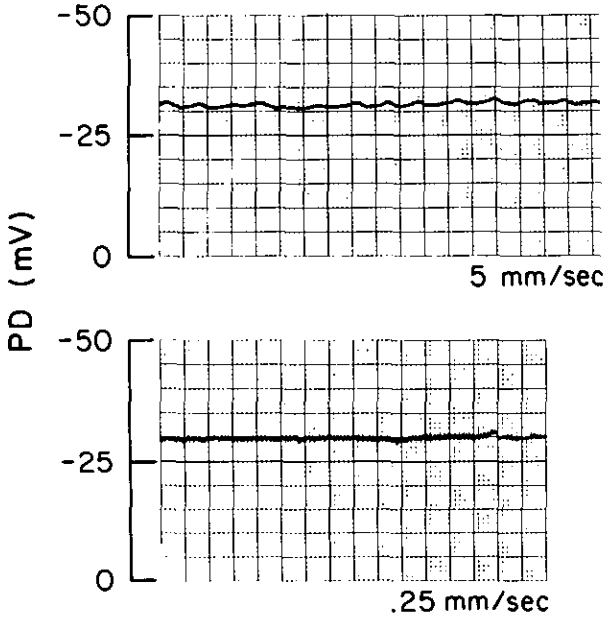

FIGURE 4. *In vivo* PD (mV) recordings from canine trachea.

To control for possible effects of liquid junction potentials between bridge perfusate and tracheal liquid, 3*M* KCl bridges were compared to the Ringer bridges employed in the fluid-filled (FF) system. In these experiments a 3*M* KCl-4% agar-filled 19 gauge needle was inserted into a subcutaneous space and a PE-160 electrode filled with 3*M* KCl-4% agar, balanced as discussed previously, was used as the exploring electrode. The values obtained with each technique were identical over a range of PDs. The correspondence of PD with the two systems suggests the effects of liquid junction are negligible.

For comparing measurements obtained with this system directly to *in vitro* measurements, excised canine trachea was mounted in Ussing chambers and PD recorded by standard techniques. Then, the chamber was detached from the *in vitro* apparatus, reference 19 gauge needle electrode inserted into the solution bathing the serosal surface of the mem-

brane, fluid evacuated from the mucosal side, and PD recorded directly by introduction of the fluid filled exploring electrode onto the mucosal membrane surface. The potentials measured with *in vitro* and *in vivo* bridges in this situation were identical ($n = 6$). These data suggest that the filtering techniques used to process the *in vivo* signals did not contribute to the measured potentials and indicate a close correspondence between *in vitro* and *in vivo* measured PD in the canine trachea.

Further, we have compared PDs measured with the fluid-filled bridge in other organs to those reported in the literature. Canine gastric PDs from three dogs were measured under fluoroscopic control. The mean PD, 54 mV, is similar to that reported by Dennis and others (*21*). Esophageal PDs in these dogs were −20 mV, with a regional PD profile similar to that reported in rabbit and man by Powell et al. (*2*).

PD was measured at three random sites in the trachea and mean value calculated. Table 4 shows the mean PD ± SE from 27 separate dogs obtained by using the FF technique, and for comparison the mean peak *in vitro* PD ± SE from the study previously cited from our laboratory. The mean tracheal PD is −29 mV, a value indistinguishable from peak *in vitro* values.

Table 4. Comparison of canine tracheal PD *in vivo* and *in vitro*.

	Tracheal transepithelial biopotential, mV[a]
In vivo	29.1 ± 3.0
In vitro	33.5 ± 2.9

[a]Mean ± SE.

The fluid-filled bridge has made it possible to assess the pharmacologic modulation of PD *in vivo* by direct addition of agents to the bridge perfusate, ensuring application of drug directly at the site of PD measurement. Drug-containing Ringer is flushed through the bridge perfusion system pump run in reverse for 1.5 min after bridge immersion in drug-free Ringer. During perfusion, the time required to clear the drug free fluid provides a control period. Drug effects were compared to a group of 10 dogs with Ringer perfusion only. An example of the effect of ouabain, $10^{-3}M$, on tracheal PD in four dogs is plotted as a function of time in Figure 5. Ouabain produces a slow reduction in PD. Both the magnitude of the change and time course resemble those reported for the *in vitro* preparation.

As the majority of the reports on pharmacologic pertubation of tracheal bioelectric properties have focused on only the effects of serosal drug addition, an appropriate comparison of *in vivo* with *in vitro* drug effects required a parallel set of experiments with excised trachea. The pattern of *in vivo* response

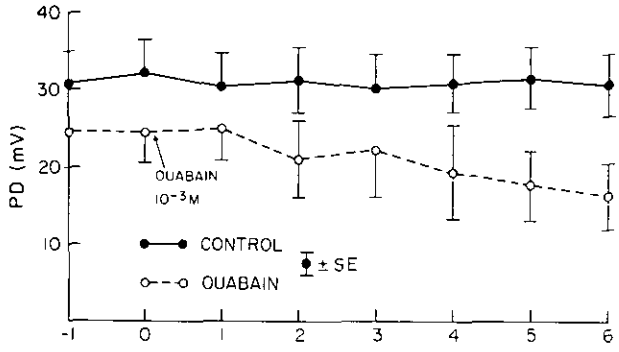

FIGURE 5. PD response to ouabain addition to mucosal surface of canine trachea: (●) control; (○) ouabain; all values ± SE.

is compared with the *in vitro* response to mucosal drug additions in Table 3. It is obvious that the pattern of response to mucosal drug application in both preparations is similar.

Hence, (1) the absence of significant liquid junction potentials (2) the similarity between PD as measured with *in vivo* and *in vitro* bridges on excised epithelium, (3) the similarity between PDs measured in other organs with the fluid filled electrodes and values in the literature, and (4) similarity in pattern of response to drug applications *in vivo* and *in vitro*, indicate that the *in vivo* tracheal PD can be measured accurately and reliably with this technique. Further, the magnitude of that PD measured by this technique implies that the low values reported by others may be in error. The technique should allow direct *in vivo* studies of the genesis and regulation of the airway biopotential in both animal and man. In regard to the interests of this symposium, effects of environmental pollutants on airway potentials *in vivo* are feasible.

The pathophysiologic implications of airway mucosal hyperpermeability likely are several. A loss of the "barrier" function would facilitate movement of inhaled materials into the airway wall. Recent studies in conjunction with Dr. J. Richardson at McGill have shown in the chicken that airway hyperpermeability induced by methacholine, enhances antibody response to antigen instilled into the trachea (*23*). This enhanced response was assumed to result from an increased antigen load. The effects of airway hyperpermeability on airway reactivity in asthmatics to naturally occurring antigens have not been evaluated. However, the hyperreactivity to inhaled chemical agonists that is a characteristic of asthmatics may, in part, be mediated by airway hyperpermeability.

It has been shown in the Ascaris-sensitive rhesus monkey and guinea pig that specific antigen challenge leads to mucosal hyperpermeability to topically applied small molecular weight polypeptides

Table 5. Comparison of *in vivo* and *in vitro* PD response in canine trachea to mucosal application of pharmacologic agents.

	Profile of PD response, % of control	
	In vivo ΔPD	*In vitro* ΔPD
Ouabain (10^{-3} *M*)	−33.5	−28.0
Amphotericin (10^{-5} *M*)	+77.0	+58.0
Acetycholine (5×10^{-4} *M*)	0	0
Atropine (10^{-3} *M*)	0	0
Histamine (10^{-3} *M*)	−10.0	+5.0

and HRP (*24, 25*). Further, the rhesus monkey demonstrates a period of hyperreactivity to inhaled histamine for an interval after antigen challenge, even after R_L has returned to baseline. Using radiolabeled histamine as a tracer, it has been observed that post-challenge airway hyperreactivity is associated with an increased fractional absorption of inhaled histamine into the blood (*26*). These data are consistent with the hypothesis that airway epithelial hyperpermeability, induced by allergic bronchoconstriction contributes to airway hyperreactivity by increasing flows of inhaled bronchoactive agents to effector sites in the airway wall. However, until experiments can be performed that alter airway permeability in the absence of changes in bronchomotor tone, the association of airway hyperpermeability and hyperreactivity cannot be taken as causal. The recent demonstration in collaboration with Dr. Richardson that viral infection in chickens increases airway permeability to HRP suggests that this mechanism may contribute to the increased airway reactivity with viral infections in humans.

A hyperpermeable mucosal surface might be expected to impair mucus clearance by two mechanisms. First, if active secretion of chloride secretion into the airway lumen is important to hydration of the airway, epithelial hyperpermeability, by increasing the passive "leak" of the chloride toward the interstitium, dissipating the osmotic gradient that drives water toward the lumen, would be expected to result in dehydration of the airway. Second, increased flows of macromolecules, e.g., albumin, through a more permeable epithelium down the chemical gradient into the airway lumen could occur, as has been reported for albumin in asthmatics (*27*). Albumin binds to mucus glycoproteins, increases crosslinking and may thereby alter viscoelastic properties and diminish mucociliary clearance.

The epithelium lining the airway appears to function as an effective, though not absolute, barrier to the movement of large hydrophilic substances between airway lumen and interstitium. The principal path of translocation for these substances across the airway mucosa appears to be paracellular. Experiments on the guinea pig are consistent with the notion that a variety of inhaled noxious agents, e.g., ether and cigarette smoke, increase epithelial permeability to HRP by increasing the flow of this probe through paracellular paths, probably by damaging the epithelial tight junctions. *In vivo* tracheal PD in dogs agrees closely with *in vitro* values and suggests the use of this technique in rapid screening for epithelial damage.

REFERENCES

1. Schneeberger-Keeley, E. E., Karnovsky, M. J. The ultrastructural basis of alveolar-capillary membrane permeability to peroxidase used as a tracer. J. Cell Biol. 37: 781 (1968).
2. Bensch, K. G., Dominguez, F., and Liebow, A. A. Absorption of intact protein molecules across the pulmonary air-tissue barrier. Science 157: 1204 (1967).
3. Theodore, J., Robin, E. D., Gaudio, R., and Acevedo, S. Transalveolar transport of large polar solutes (sucrose, inulin, and dextran). J. Appl. Physiol. 129: 989 (1975).
4. Richardson, J. B., Hogg, J. C., Bouchard, T., and Hall, D. L. Localization of antigen in experimental bronchoconstriction in guinea pigs. J. Allergy Clin. Immunol. 52: 172 (1973).
5. Richardson, J., Bouchard, T., and Ferguson, C. C. Uptake and transport of exogenous proteins by respiratory epithelium. Lab. Invest. 35: 307 (1976).
6. Inoue, S., and Hogg, J. C., A freeze-etch study of the tracheal epithelium of normal guinea pigs with particular reference to intercellular junctions. J. Ultrastruct. Res. 61: 89 (1977).
7. Boucher, R. C., Ranga, V., Pare, P. D., Inoue, S., Moroz, L. A., and Hogg, J. C. Effect of histamine and methacholine on guinea pig tracheal permeability to HRP. J. Appl. Physiol. Resp. Environ. Exercise Physiol. 45: 939 (1978).
8. Rhodes, R. S., and Karnovsky, M. J. Loss of macromolecular barrier function associated with surgical trauma to the intestine. Lab. Invest. 25: 220 (1971).
9. Simani, A. S., Inoue, S., and Hogg, J. C. Penetration of the respiratory epithelium of guinea pigs following exposure to cigarette smoke. Lab. Invest. 31: 75-81 (1974).
10. Johnson, J., Boucher, P. C., Inoue, S., Moroz, L. A., and Hogg, J. C. The effect of graded doses of whole cigarette smoke on respiratory mucosal permeability (abstract). Am. Rev. Resp. Dis. 117: 244 (1978).
11. Bienenstock, J., Rudzik, O., Clancy, R. L., et al. Bronchial lymphoid tissue. In: The Immunoglobulin A System (J. Mestecky and A. R. Lawton III, Eds., Plenum Press, New York and London, 1974, pp 47-56.
12. Michel, R. P., Inoue, S., and Hogg, J. C. Pulmonary capillary permeability to HRP in dogs: a physiologic and morphologic study. J. Appl. Physiol. 42:13 (1977).
13. Olver, P. E., Davis, B., Marin, M. G., and Nadel, J. A. Active transport of Na^+ and Cl^- across the canine tracheal epithelium *in vitro*. Am. Rev. Resp. Dis. 122: 811 (1975).
14. Boucher, R. C., Gatzy, J. T. Tracheal epithelial permeability to nonelectrolytes (abstract). Physiologist 21: 11 (1978).
15. Marin, M. G., Davis, B., and Nadel, J. A. Effect of acetylcholine on Cl^- and Na^+ fluxes across dog tracheal epithelium *in vitro*. Am. J. Physiol. 231: 1546 (1976).
16. Solomon, A. K. Characterization of biological membranes by equivalent pores. J. Gen. Physiol. 51: 3355 (1968).
17. Diamond, J. M. Channels in epithelial cell membranes and junctions. Fed. Proc. 37: 2639 (1978).
18. Pennington, J. E., and Reynolds, H. Y. Concentrations of gentamicin and carbenicillin in bronchial secretions. J. Infect. Dis. 128: 63 (1973).
19. Hale, K., Sandler, L., and Niewoehner, D. Sensitivity of the

in vivo transmucosal potential difference to beta-adrenergic agents. Clin. Res. 26: 447A (1978).
20. Boucher, R. C., Bromberg, P. A., and Gatzy, J. T. Measurement of the *in vivo* electrical potential difference in canine trachea with a fluid filled bridge. Clin. Res. 26: 802A (1978).
21. Dennis, W. H. Potential difference across the pyloric antrum. Am. J. Physiol. 197:19 (1959).
22. Turner, K. S., Powell, D. W., Carney, C. N., Orlando, R. C., and Bozymski, E. M. Transmural electrical potential difference in the mammalian esophageal *in vivo*. Gastroenterology 75: 286 (1978).
23. Boucher, R. C., and Richardson, J. Unpublished data.
24. Boucher, R. C., Pare, P. D., and Hogg J. C. Relationship between bronchial hyperreactivity and hyperpermeability to histamine in ascaris sensitive monkeys. J. Allergy Clin. Immunol. 64: 197 (1979).
25. Boucher, R. C., Pare, P. D., Gilmore, N., Moroz, L. A., and Hogg, J. C. Airway mucosal permeability in the ascaris suum-sensitive rhesus monkey. J. Allergy Clin. Immunol. 60: 134 (1977).
26. Boucher, R. C., Ranga, V., Pare, P. D., Moroz, L. A., and Hogg, J. C. The effect of allergic bronchoconstriction on respiratory mucosal permeability. Physiologist 20: 11 (1977).
27. Dunnill, M. S. The pathology of asthma, with special reference to changes in the bronchial mucosa. J. Clin. Pathol. 13: 27 (1960).